

# Fracture Behavior of the Heat-Affected Zone in 5% Ni Steel Weldments

*Although the use of 5% Ni steel appears satisfactory for LNG applications where the service temperature is approximately 111 K, the fracture resistance of 5% Ni steel may be significantly lower than expected based on previous investigations.*

BY H. I. MCHENRY AND R. P. REED

**ABSTRACT.** The fracture properties of the base metal and the heat-affected zone (HAZ) of 5% Ni steel weldments were determined at room temperature, 111 K (-260 F) and 76 K (-323 F); emphasis was placed on tests at 111 K, the minimum boiling point of liquefied natural gas (LNG). The 32 mm (1¼ in.) thick test plates, which met the requirements of ASTM A645, were welded using the pulsed-power gas metal arc process at a heat input of 10.6 kJ/cm. The fatigue crack growth rates were determined for cracks growing through the thickness using four-point bend specimens. At 111 K, the rates in the base metal were essentially the same as found by other investigators; however, the rates in the HAZ were up to 10 times faster than previously reported.

Fracture toughness tests were conducted under load-controlled conditions using J-integral procedures. At 111 K, the base metal and HAZ toughness values were 30 and 50% lower, respectively, than toughness values obtained previously for the same plate of test material under displacement-controlled conditions.

Fracture mechanics analyses using the results reported herein indicate that 5% Ni steel is suitable for LNG applications, but more conservative estimates of fatigue life and critical crack size are necessary.

## Introduction

The international trade in liquefied natural gas (LNG) has created a large

market for equipment to transport, store and process LNG. Structural materials used for these applications must have adequate strength and toughness at 111 K (-260 F), the minimum boiling point of LNG. Presently, 9% Ni steel (ASTM A353 and A553) and 5083-0 aluminum alloy are the most widely used materials for LNG structural applications.<sup>1</sup> However, a 5% Ni steel, which is specially heat treated to meet the requirements of ASTM specification A645, offers significant cost savings potential and may be widely used in the future.

Over the past few years, considerable work has been done to characterize 5% Ni steel and its weldments at temperatures down to 76 K (-323 F).<sup>2</sup> The fatigue and fracture properties of the weldments have been evaluated by Sarno, Bruner and Kampschafer;<sup>3</sup> Bucci, Greene and Paris;<sup>4</sup> and Murayama, Pense and Stout.<sup>5</sup> The fatigue crack growth behavior in the heat-affected zone (HAZ) was found<sup>3,4</sup> to be far superior to the corresponding behavior in the base metal. For example, at a stress intensity range,  $\Delta K$ , of 40 MPa  $\sqrt{\text{m}}$  (36.1 ksi  $\sqrt{\text{in.}}$ ), the growth rates of cracks in the base metal were about 10 times faster than that of cracks in the HAZ.

The fracture toughness of the HAZ

was reported<sup>3-5</sup> to range between 88 and 526 MPa  $\sqrt{\text{m}}$  (79.4 to 475 ksi  $\sqrt{\text{in.}}$ ) over a thickness range of 6.4 to 38 mm (¼ to 1½ in.); low values occurred in thick-section load-controlled tests<sup>3</sup>, and the highest values occurred in thin-section displacement-controlled tests. This variation in toughness results in a 36-fold difference in calculations of critical crack lengths.

The present study was undertaken to further investigate and clarify the fracture behavior of 5% Ni steel weldments. Fatigue and fracture tests were conducted on the HAZ and the base metal at room temperature, 111 K and 76 K. Emphasis was placed on determining the relative contributions of material variability and of test-method peculiarities to the range of results previously reported. The questions of principal interest are:

1. Is the fatigue crack growth resistance of the HAZ really that good?

2. Is the toughness of the HAZ really that unpredictable?

To answer these questions, two experimental objectives were established. First, the fatigue crack growth behavior of a crack in the HAZ will be determined as it propagates through the thickness. In addition to being an important practical case, cracks in this orientation do not benefit from the favorable closure effects that may have influenced the previous results as discussed by Bucci *et al.*<sup>4</sup> Second, the range of fracture toughness in the HAZ will be established under load-controlled conditions. A direct com-

H. I. MCHENRY and R. P. REED are with the Cryogenics Division, Institute for Basic Standards, National Bureau of Standards, U. S. Department of Commerce, Boulder, Colorado.

**Table 1—Properties of the 5% Ni Steel Base Metal**

*Chemical composition, %<sup>a</sup>*

		C	Mn	P	S	Si	Ni	Mo	Al	N
ASTM-A645	Min	—	.30	—	—	.20	4.75	.20	.05	—
	Max	.13	.60	.025	.025	.35	5.25	.35	.12	.02
Heat analysis		.08	.60	.010	.009	.25	5.03	.30	.08	.010

*Tensile properties<sup>a</sup>*

Temperature, K	Orientation	Yield Strength, MPa (ksi)	Ultimate Strength, MPa (ksi)	Elongation, %	Reduction of area, %
297	Longitudinal	514 (74.6)	676 (98.1)	33	74
297	Transverse	507 (73.6)	678 (98.4)	33	77
144	Transverse	563 (81.7)	930 (135.0)	30	72
76	Transverse	772 (112.0)	1137 (165.0)	34	66

*Charpy impact toughness<sup>a</sup>*

Temperature, K	Orientation	Individual values, J			Average, J	(Ft-lb)
		111	Longitudinal	114	144	124
111	Transverse	84	91	97	91 (67)	
103	Longitudinal	82	72	—	77 (56)	
103	Transverse	79	79	—	79 (58)	
76	Longitudinal	50	46	60	52 (38)	
76	Transverse	48	49	31	42 (31)	

*Elastic properties<sup>a</sup>*

Temperature, K	Young's Modulus, E GPa (10 <sup>6</sup> psi)	Poisson's ratio, $\gamma$
297	198 (28.7)	0.288
111	208 (30.2)	0.282
76	209 (30.3)	0.281

parison with the displacement-controlled toughness measured by Sarno et al<sup>3</sup> will be possible because the test weldment was prepared using 5% Ni steel from the same heat and essentially the same welding procedures.

**Materials and Procedures**

**Test Weldments**

Two 32 mm (1¼ in.) thick 5% Ni steel plates were welded with Inconel 92 (AWS A 5.14 Class ERNiCrFe-6) filler metal. One of the test plates was oriented with the rolling direction perpendicular to the weld joint. This enabled evaluation of HAZ toughness in both base-metal orientations. The chemical composition and mechanical properties of the base metal as reported by Sarno<sup>4</sup> are shown in Table 1.

Welding was done by the Armco Steel Research Center using the pulsed-power gas metal-arc process and the parameters summarized in Table 2. The weld-joint preparation and the welding sequence are shown in Fig. 1.

Charpy impact tests were conducted to verify that the weldment met the toughness requirements established by the U.S. Coast Guard<sup>5</sup> for LNG service. Type A (V-notch) specimens were tested in accordance with ASTM E-23 at 76 K (-323 F). The specimens

**Table 2—Welding Procedures**

Weld position	Horizontal		
Plate thickness	32 mm (1¼ in.)		
Joint design	Double vee (See Fig. 1)		
Shielding gas	75He-25Ar at 39 liters/second		
Interpass temp	38 C maximum		
No. of passes	21		
Filler metal diameter	1.1 mm (0.04 in.)		
Parameters:	Pass 1	Pass 2	Passes 3-21
Current, DCRP, A	110	140	140
Voltage, V	30	32	32
Travel, mm/sec (ipm)	3.4(8)	5.1(12)	4.2(10)
Heat input, kJ/cm (kJ/in.)	9.8(24.8)	8.8(22.4)	10.6(26.9)

were cut transverse to the weld axis with the notches normal to the plate surface. The HAZ specimens were cut such that the notch was in the base metal oriented with the rolling direction parallel to the weld joint. Three specimens were tested for each of the following locations as shown in Fig. 2: centered in the weld metal; on the fusion line; and in the HAZ 1, 3 and 5 mm from the fusion line. The results are summarized in Table 3.

**Fatigue Crack Growth Specimens**

The fatigue crack growth tests were conducted using four-point bend specimens as shown in Fig. 3. This specimen was selected to enable determination of the fatigue crack growth rates in the L S orientation, i.e.,

the plate is loaded in the transverse direction, and the crack propagates through the thickness.

A compliance calibration, needed for crack length measurements in the fatigue tests, was established for the four-point bend specimen. Compliance, C, is the ratio of crack opening displacement,  $\Delta$ , to applied load, P; and C is a function of crack length, a, specimen geometry, and the elastic modulus of the material, E:

$$C = \Delta/P = (1/EB)f(a/W) \quad (1)$$

where B = specimen thickness, W = specimen width, and f(a/W) = compliance function.

The compliance calibration, EBC vs. a/W, was obtained using a single spec-

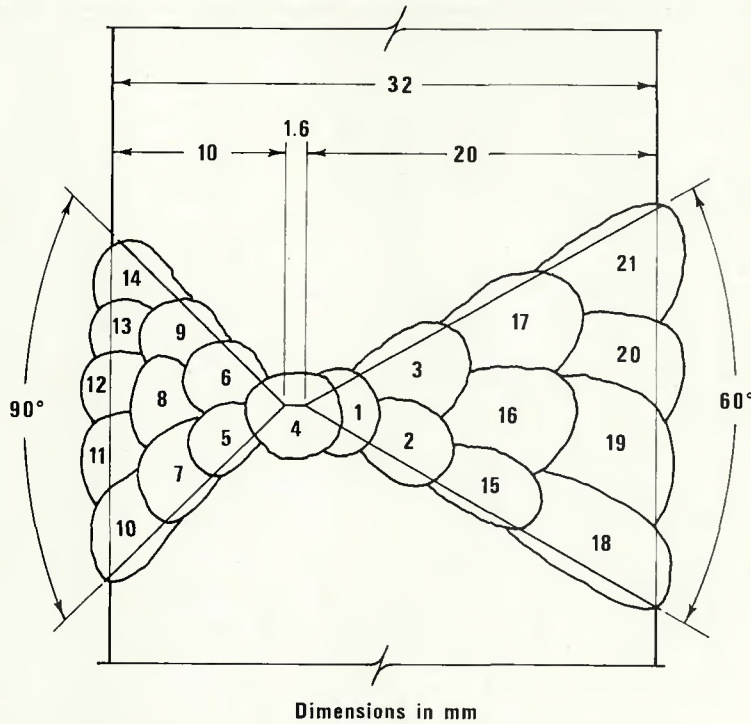


Fig. 1—Weld joint preparation and welding sequence (25.4 mm = 1 in.)

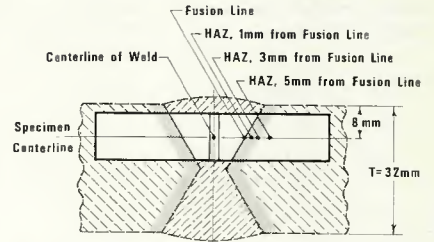


Fig. 2—Notch locations for Charpy impact specimens (25.4 mm = 1 in.)

imen by progressively extending a fatigue crack into the specimen and measuring compliance at growth increments of approximately 1 mm (0.04 in.). After each compliance measurement, the ratio of minimum-to-maximum load,  $R$ , was changed to either  $R = 0.1$  or  $R = 0.5$ . An ASTM E-399 clip gage was used for  $\Delta$  measurements. At a crack length of 1.81 cm, the specimen was fractured to expose the fatigue bands corresponding to each increment of crack growth. Crack lengths for each compliance measurement point were measured from a photograph (Fig. 4) of the fracture surface. An average value of the mid-thickness and two quarter-thickness readings was used as the crack length.

The results of the compliance calibration test are shown in Fig. 5. A least-squares best-fit analysis of the data yields the following expression:

$$a = W[0.5332 - 1.863(\text{EBC})^{1/6} + 1.641(\text{EBC})^{1/3} - .3525(\text{EBC})^{1/2}] \quad (2)$$

for  $0.2 \leq a/W \leq 0.6$ .

The agreement of equation (1) with the experimental data and the theoretical results of Srawley and Gross<sup>9</sup> is shown in Fig. 5.

#### Fatigue Crack Growth Testing

Fatigue crack growth tests were conducted on the base metal and the HAZ in air at room temperature, in nitrogen vapor at 111 K and in liquid nitrogen at 76 K. Two tests at 76 K were also conducted on the weld metal. The LNG temperature of 111 K was maintained within  $\pm 3$  K ( $\pm 5.4$  F) by adjusting the flow of liquid nitrogen

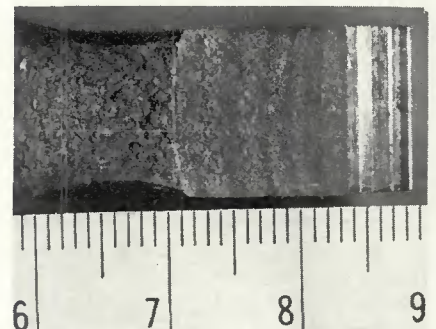


Fig. 4—Fracture surface of the compliance calibration specimen (scale in cm)

Table 3—Results of the Charpy V-Notch Impact Tests

Notch Location (see Fig. 2)	Absorbed Energy	
	Individual tests, J	Average, J (ft-lb)
Weld metal	Failed to break (FTB)	FTB
Fusion line	109, 91, 91	97(71)
HAZ, 1 mm (0.04 in.)	159, 91, 126	125(92)
HAZ, 3 mm (0.12 in.)	113, 31, FTB	88(65)
HAZ, 5 mm (0.20 in.)	84, 54, 94	77(57)

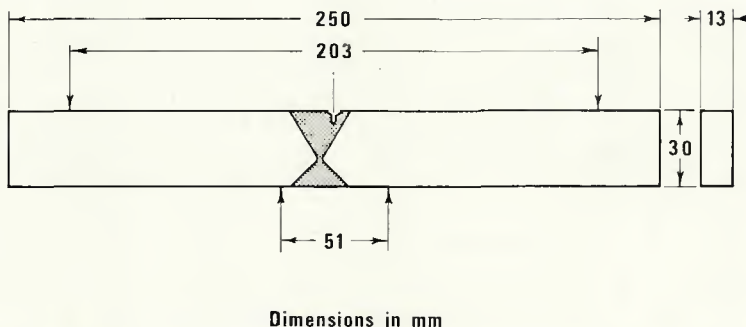
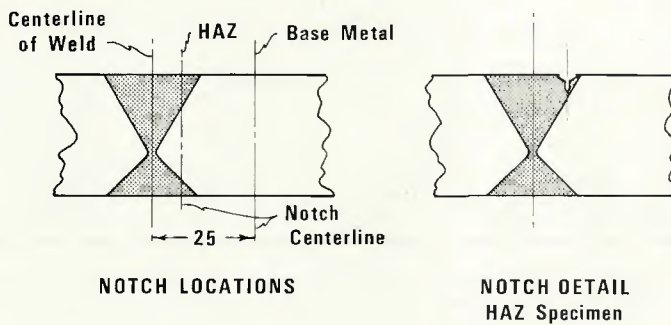


Fig. 3—Four-point bend specimen for fatigue crack growth tests (25.4 mm = 1 in.)

into the test dewar with a hand-operated needle valve. Temperature was monitored with a type E thermocouple taped to the bottom of the test specimen.

Four-point bend specimens were mounted in the test fixture shown in Fig. 6 for fatigue testing in a 100 kN (22,480 lb) electrohydraulic fatigue machine. Tests were conducted using a 20 Hz sinusoidal load wave at an R of 0.1. All specimens were precracked at room temperature to an initial crack length of 0.611 cm or 1/4 in. (i.e., 0.311 cm or 1/8 in. beyond the machined-notch depth) using a maximum load that was less than or equal to the maximum load for the fatigue crack growth tests. The procedures for room and cryogenic testing were the same except for the temperature control provisions.

The compliance method<sup>9</sup> was used for crack length measurements. Compliance measurements were taken at increments where the estimated growth was 0.751 cm. The recorded data were cycle number and compliance. Crack lengths were determined from the compliance calibration, equation (1). Stress intensity ranges,  $\Delta K$ , were computed from the K-calibration equation of Gross and Srawley<sup>10</sup>:

$$\Delta K = [(P_{\max} - P_{\min})\sqrt{a/BW}]Y(a/W) \quad (3)$$

where,

$$Y(a/W) = 1.992 - 2.468(a/W) + 12.97(a/W)^2 - 23.17(a/W)^3 + 24.8(a/W)^4 \quad (4)$$

$P_{\max}$  = maximum load in the fatigue cycle, and  $P_{\min}$  = minimum load in the fatigue cycle. Crack growth rates were determined by the central difference method. The results were presented in log-log plots of  $da/dN$  vs.  $\Delta K$ .

### Fracture Toughness Testing

Fracture toughness tests were conducted on the base metal and the HAZ in nitrogen vapor at 111 K. Additional tests were conducted on the HAZ in air at room temperature and in liquid nitrogen at 76 K. The temperature of 111 K was maintained as in the fatigue tests except that the control thermocouple was mounted on the side of the specimen in the plane of the crack.

Modified compact specimens (Fig. 7) were tested in accordance with the J-integral procedures described by Landes and Begley.<sup>11</sup> In this method, each specimen is loaded to a predetermined displacement level such that a range of subcritical crack extensions occurs in a given test series.

Upon reaching the predetermined displacement level, the specimen is unloaded, heat tinted to mark the

region of subcritical crack growth that occurred during the load cycle and subsequently loaded to failure to expose the fracture surfaces for measurements of crack length,  $a$ , and crack extension,  $\Delta a$ . The J-integral value for the test is calculated using the approximation of Rice, Paris and Merkle:<sup>12</sup>

$$J = 2A/B(W-a) \quad (5)$$

where  $A$  is the area under the load displacement curve.

For a given test series, a curve of  $J$  vs.  $\Delta a$  is constructed. On the same graph, the line defined by equation (6) is drawn:

$$J = 2\sigma_{f_{low}}\Delta a \quad (6)$$

where  $\sigma_{f_{low}} = (\sigma_{ys} + \sigma_{utS})/2$ ,  $\sigma_{ys} = 0.2\%$  offset yield strength, and  $\sigma_{utS} =$  ultimate tensile strength. The intersection of the  $J$ - $\Delta a$  plot and the  $J/2\sigma_{f_{low}}$  line is defined as  $J_{IC}$ , the value of  $J$  at the onset of crack extension. Apparent crack extension at  $\Delta a$  values less than  $J/2\sigma_{f_{low}}$  is attributed to deformation at the crack tip instead of material separation. Begley and Landes<sup>13</sup> have proposed that the plane strain fracture toughness,  $K_{IC}$ , is related to  $J_{IC}$  as follows:

$$K_{IC}(J) = (J_{IC}E/1-\gamma^2)^{1/2} \quad (7)$$

where  $E$  is Young's modulus and  $\gamma$  is Poisson's ratio.

Tests were conducted in two electrohydraulic fatigue machines, each with 100 kN (22,480 lb) capacity. One machine employed the cryostat described by Fowlkes and Tobler<sup>14</sup>, and the other a dewar equipped with the mechanical feedthrough shown in Fig. 8. The specimens were loaded at 0.5 kN/s (111 lb/s) under load control. Loading was continued until either failure, crack extension due to pop-in, or a predetermined displacement was reached.

The specific test termination point for each test is noted in the results. Specimens unloaded prior to failure were heat tinted and subsequently loaded to failure at 76 K to expose the fracture surface. Tinting was accomplished by heating the specimens in a 813 K furnace for 15 minutes. The fractured surfaces were visually examined under  $\times 35$  magnification for evidence of subcritical crack extension.

## Results and Discussion

### Fatigue Crack Growth

The fatigue crack growth test results on 5% Ni steel weldments at room temperature, 111 K and 76 K are summarized in Figs. 9-11, respectively. The Paris power law<sup>15</sup>, equation (8), is used as the basis for empirical analysis of the data:

$$da/dn = C(\Delta K)^n \quad (8)$$

where  $C$  is the intercept and  $n$  is the slope of a log-log plot of  $da/dn$  vs.  $\Delta K$ .

A least-squares regression analysis was used to obtain a statistical fit of the crack growth data. For each test

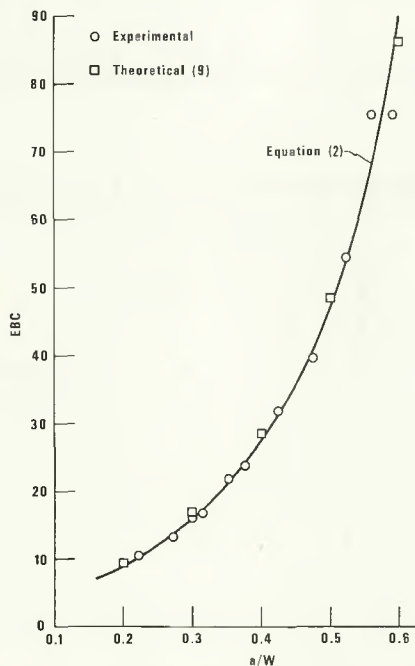


Fig. 5—Compliance calibration of the four-point bend specimen

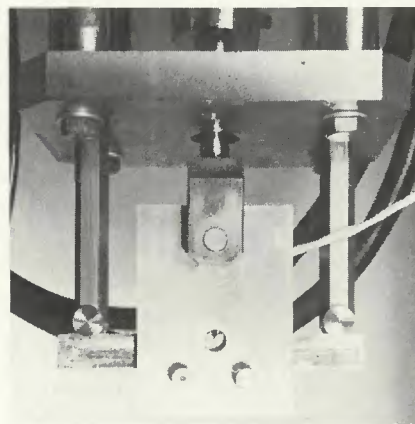


Fig. 6—Four-point bend test fixture

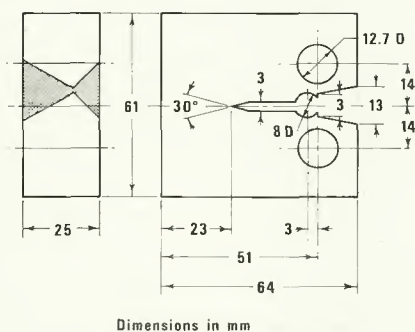


Fig. 7—Modified compact specimen showing notch location for HAZ tests (25.4 mm = 1 in.)

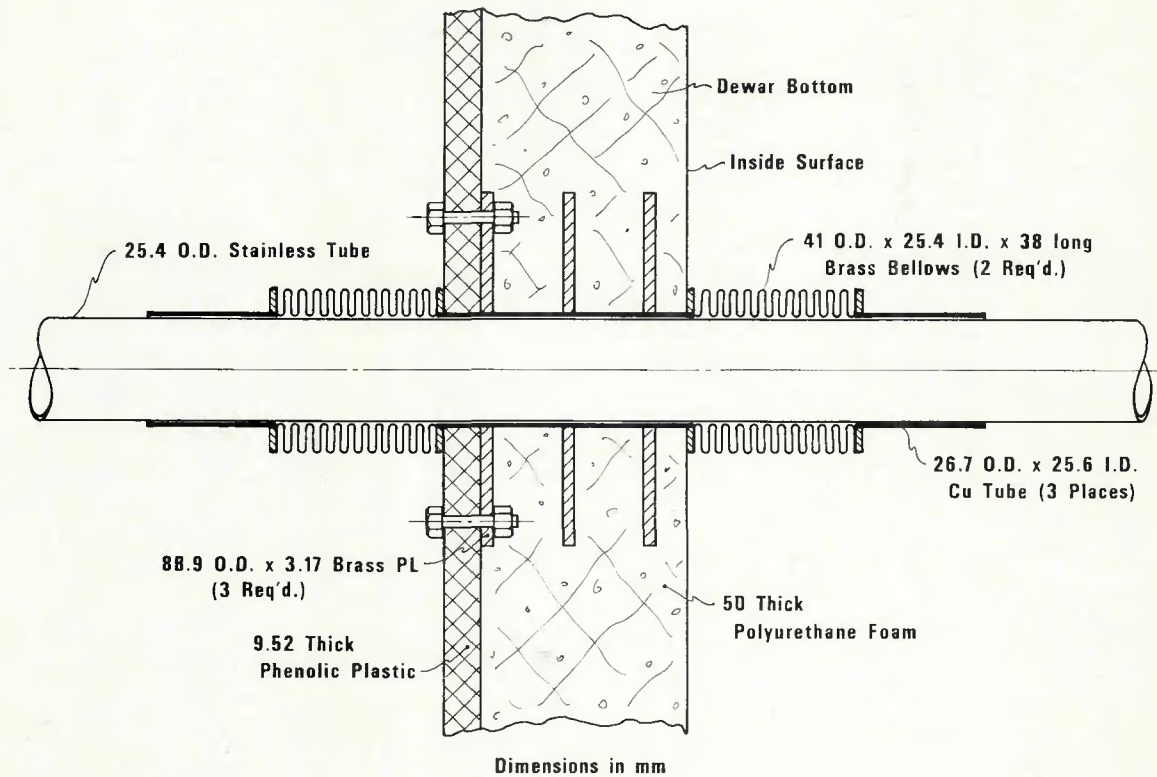


Fig. 8—Mechanical feedthrough for test dewar

condition, values of  $C$  and  $n$  are included in the appropriate plot of the results—Figs. 9 to 11.

In all cases, the fatigue cracks propagated in a direction perpendicular to the bending stress, i.e., local properties within the HAZ did not influence the path followed by the fatigue crack. The location of the crack tip varied from the fusion line to a distance about 7 mm (0.28 in.) from the fusion line as the crack propagated through the thickness.

The fatigue crack growth data for the base metal and the HAZ at room temperature are summarized in Fig. 9. The growth rates are essentially the same in both cases and coincide with the base metal data of Buccì et al.<sup>4</sup> and of Tobler, Mikesell, Durcholz and Reed.<sup>16</sup>

The fatigue crack growth data for the base metal and the HAZ at 111 K are summarized in Fig. 10. The base metal data are in good agreement with the data of previous investiga-

tions.<sup>3,11,16</sup> However, in contrast with previous results<sup>3,4</sup> where the HAZ exhibited reduced growth rates, the growth rates in the HAZ are approximately 1.5 times faster than the corresponding rates in the base metal.

The principal difference between the present and previous investigations was crack orientation. In this study, growth rates were measured as the crack propagated through the thickness; in the previous studies, through-thickness cracks were propa-

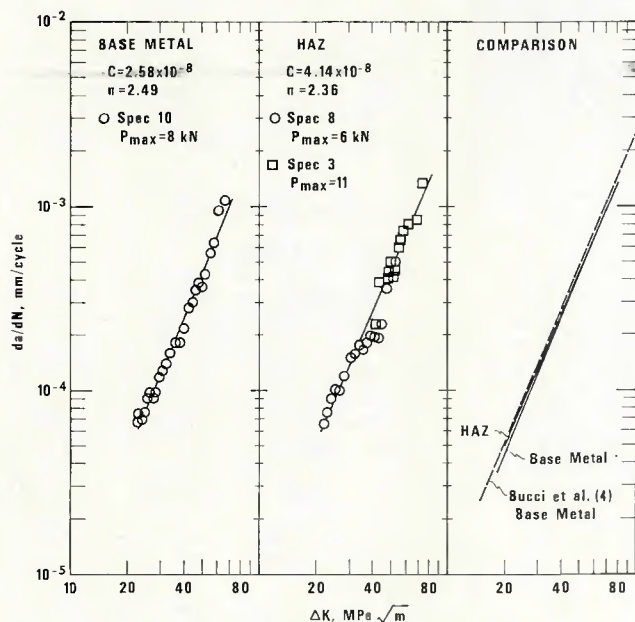


Fig. 9—Fatigue crack growth behavior of 5% Ni steel weldments at room temperature

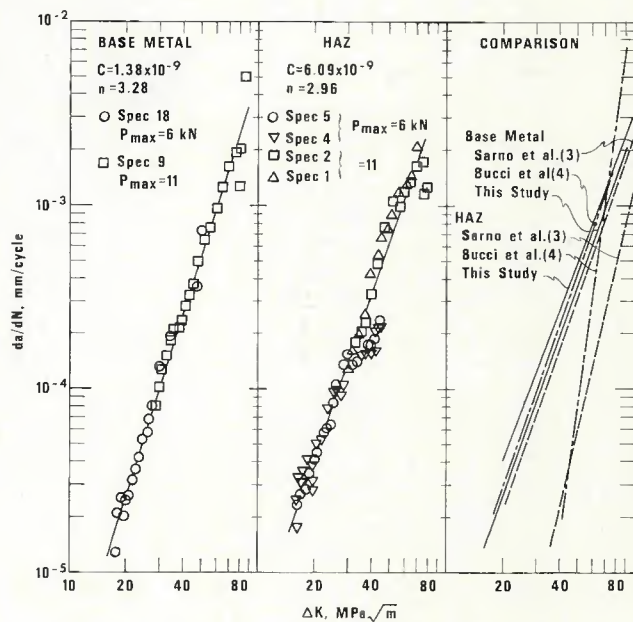


Fig. 10—Fatigue crack growth behavior of 5% Ni steel weldments at 111 K (-260 F)

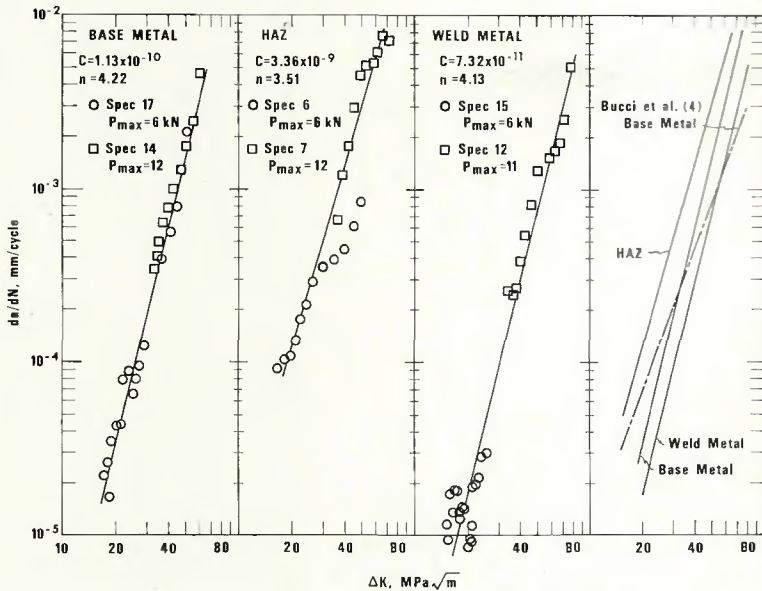


Fig. 11—Fatigue crack growth behavior of 5% Ni steel weldments at 76 K (–323 F)

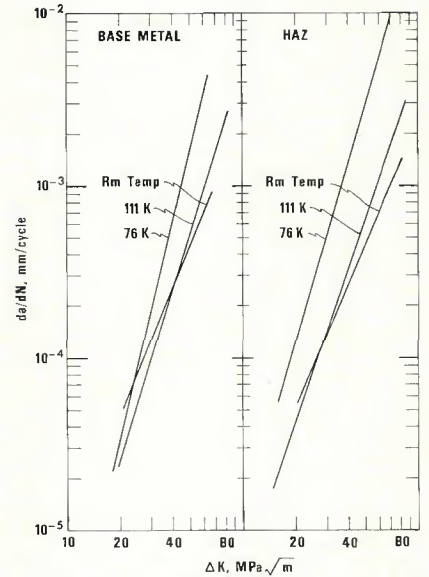


Fig. 12—Effect of temperature on the fatigue crack growth rates in 5% Ni steel weldments

gated in the rolling direction. The difference in crack orientation did not appear to influence the base metal results—which were equivalent in all cases.<sup>3,14,16</sup> However, in the previous (3,4) HAZ tests, through-thickness cracks were partially located (i.e., near both surfaces) in ductile weld metal. Apparently, deformation of the weld metal limited the range of crack-opening-displacements in these tests and resulted in reduced growth rates as discussed by Bucci *et al.*<sup>4</sup>

The fatigue crack growth data for the base metal, the HAZ and the weld metal at 76 K are summarized in Fig. 11. The base metal data overlap the results of Tobler *et al.*<sup>16</sup> but have a slightly greater slope than the results of Bucci *et al.*<sup>4</sup> The crack growth rate in the HAZ was significantly faster than that observed in the base metal. The weld metal had the greatest resistance to fatigue crack growth at 76 K—the only temperature where the crack growth behavior of the weld metal was determined. The crack growth rates in the weld metal at low  $\Delta K$  levels exhibited more scatter than observed in the higher  $\Delta K$  tests; however, growth was observed at  $\Delta K$  levels down to 15 MPa  $\sqrt{m}$  (13.5 ksi  $\sqrt{in.}$ ).

The lowest values of  $\Delta K$  employed in the weld metal tests of Sarno *et al.*<sup>3</sup> were approximately 30 MPa  $\sqrt{m}$  (27.1 ksi  $\sqrt{in.}$ ); difficulties were encountered in getting uniform crack growth along the crack front at lower stress intensities. Similarly, Bucci *et al.*<sup>4</sup> found it difficult to sustain crack growth in the weld metal at  $\Delta K$  levels less than 40 MPa  $\sqrt{m}$  (36.1 ksi  $\sqrt{in.}$ ).

The temperature dependence of fatigue crack growth in 5% Ni weldments is summarized in Fig. 12. The

room temperature and 111 K data tend to be approximately the same. A significant increase in growth rates occurred at 76 K, particularly in the HAZ tests. The relatively strong temperature dependence between 111 and 76 K may be due to the large decrease in fracture toughness that occurs over this same temperature range.<sup>16</sup>

Some crack growth retardation was observed in the present study. In each of the HAZ tests conducted at a maximum load of 6 kN (1350 lb) (specimens 8, 4, 5 and 6), retardation was exhibited at stress intensity levels of over 30 MPa  $\sqrt{m}$  (27.1 ksi  $\sqrt{in.}$ ), i.e., at crack lengths in excess of  $a/W = 0.5$ . Examination of the load-displacement curves for these data points suggest that the reduced growth rates may have been due to crack closure effects. The data points that may have been influenced by closure effects are plotted in Figs. 9 to 11; however, these data were not included in the regression analysis to determine C and n values.

Similar retardation effects were not observed in the higher load tests ( $P_{max} > 6$  kN), probably because net section yielding tended to separate the fracture surfaces at crack depths greater than  $a/W = 0.5$ .

#### Fracture Toughness

The fracture toughness data for 5% Ni steel weldments at room temperature, 111 K and 76 K are summarized in Table 4. Tests at room temperature and 76 K were conducted on the HAZ in the transverse (TL) orientation. Tests at 111 K were conducted on the base metal in the TL orientation and on the HAZ in both the longitudinal (LT) and TL orientations. Tests were not con-

ducted on the nickel-base weld metal because it was assumed to be tougher than the base metal or the HAZ on the basis of the Charpy impact results of Table 3.

Emphasis was placed on determining the range of fracture toughness characteristic of HAZ at 111 K. The upper bound was established by the base metal toughness which averaged 159 MPa  $\sqrt{m}$  (144 ksi  $\sqrt{in.}$ ) in the two specimens that were loaded to failure; the specimens unloaded prior to failure are discussed below. A lower bound was established by measuring the fracture toughness at pop-in.

Pop-in is an abrupt sub-critical crack extension that causes a discontinuity in the load-displacement curve—usually a sudden increase in displacement at a fixed or decreasing load. Three TL specimens exhibited pop-in at an average toughness of 108 MPa  $\sqrt{m}$  (97.5 ksi  $\sqrt{in.}$ ), and one LT specimen exhibited a pop-in at 136 MPa  $\sqrt{m}$  (123 ksi  $\sqrt{in.}$ ). In each test where pop-in occurred, the specimen was unloaded immediately after pop-in, heat tinted, fractured and visually examined to identify the location in the HAZ where pop-in occurred.

The fracture surfaces of the four specimens that exhibited pop-in are shown in Fig. 13. In each case, pop-in occurred along the crack front from the fusion line to a location approximately corresponding to the 5 mm (0.2 in.) line of Fig. 2. Thus, the lowest toughness region of the weldment was identified as the HAZ, but within the HAZ the location of minimum toughness could not be identified. The HAZ toughness was greater in the LT orientation, averaging 155 MPa  $\sqrt{m}$  (140 ksi  $\sqrt{in.}$ ) than in the TL orientation

**Table 4—Fracture Toughness of 5% Ni Steel Weldments**

Temperature, K	Specimen			J		K <sub>IC</sub> (J)		Notes
	No.	Type	Orientation	kJ/m <sup>2</sup>	in.-lb/ in. <sup>2</sup>	MPa √m	ksi √in.	
297	1-1	HAZ	T L	113.0	644	—	—	Unloaded, no Δa
	2-1			783.0	4468	—	—	Unloaded, no Δa
	3-1			357.0	2040	—	—	Δa = 0.457 mm
	4-1			227.0	1295	—	—	Unloaded, no Δa
111	1-4	HAZ	L T	80.7	461	—	—	Unloaded, no Δa
	2-4			85.6	489	—	—	Unloaded, no Δa
	3-4			121.0	691	—	—	Unloaded, no Δa
	4-4			109.0	620	158.0	143.0	Pop-in
	5-4			104.0	595	155.0	140.0	Pop-in
111	1-3	HAZ	T L	53.9	308	112.0	101.0	Pop-in
	2-3			87.2	498	—	—	Unloaded, no Δa
	3-3			91.1	520	145.0	131.0	Load to failure, no pop-in
	4-3			51.0	291	108.0	97.7	Pop-in
	5-3			45.9	262	103.0	92.7	Pop-in
	6-3			61.6	352	118.0	107.0	Load to failure, no pop-in
76	1-2	HAZ	T L	26.4	151	77.9	70.4	Pop-in
	2-2			19.3	110	66.6	60.2	Pop-in
	3-2			30.5	174	83.7	75.6	Load to failure, no pop-in
	4-2			20.1	115	68.1	61.5	Pop-in
	5-2			34.1	195	—	—	Unloaded, no Δa
111	3-A	Base Metal	T L	99.1	566	—	—	Unloaded, no Δa
	3-B			66.7	381	—	—	Unloaded, no Δa
	3-C			135.0	770	—	—	Unloaded, no Δa
	3-D			112.0	641	161.0	145.0	Load to failure, no pop-in
	3-E			56.4	322	—	—	Unloaded, no Δa
	3-F			108.0	619	157.0	142.0	Load to failure, no pop-in

which averaged 131 MPa √m (118 ksi √in.).

The HAZ of 5% Ni weldments exhibited relatively brittle behavior at 76 K and very tough behavior at room temperature. The toughness at 76 K averaged 77 MPa √m (69.5 ksi √in.). Three of the five tests at 76 K satisfied the thickness requirements of ASTM Standard E-399 for valid K<sub>IC</sub> measurements.

The toughness of the HAZ at room temperature could not be estimated on the basis of the four tests conducted because subcritical crack growth occurred in only one test. The results do suggest that the HAZ toughness is at least as good as the base metal toughness of 220 MPa √m (200 ksi √in.) reported by Tobler et al.<sup>16</sup> for a test plate from the same heat of 5% Ni steel.

In the fracture toughness tests, efforts were made to obtain J-Δa data for K<sub>IC</sub>(J) calculations as described in the procedure section. However, subcritical crack extension was not detected (except in room temperature test 3-1) prior to pop-in or fracture despite repeated efforts to find it.

In Table 4, each specimen with the note "unloaded, no Δa" was loaded to the J level given, unloaded, heat tinted, fractured, and visually examined at ×35 for evidence of subcritical crack extension; in each test as noted, no crack extension was observed. Apparently 5% Ni steel (base metal and HAZ) does not exhibit the slow tearing type of subcritical crack exten-

sion at temperatures of 111 K and 76 K unless tested by the displacement-controlled R-curve method used by Sarno et al.<sup>3</sup> Tobler et al.<sup>16</sup> did obtain J-Δa curves at room temperature and 195 K but did not report subcritical crack growth in the 111 K and 76 K tests.

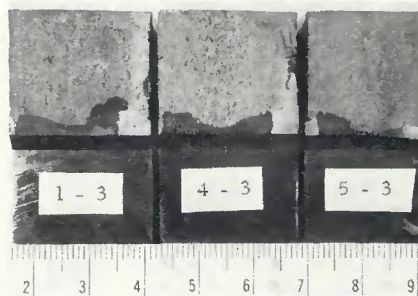


Fig. 13—Fracture surfaces of the HAZ specimens that exhibited pop-in at 111 K (-260 F)

The plane of the notch in the HAZ specimens is shown in the sketch of the fracture toughness specimen—Fig. 7. The fatigue precrack did not propagate uniformly in the HAZ, growing faster on the outside than in the center. The characteristic shape of the precrack, as shown in Fig. 13, was essentially the same in all HAZ tests. Crack lengths for fracture toughness calculations were arbitrarily defined as the average of the two maximum lengths at the outside and the minimum length in the center. The precracks in the base metal tests were

uniform, and the length was computed as the average of the ¼, ½ and ¾ thickness values.

Care must be taken in comparing the present results with those obtained by Sarno et al.<sup>3</sup> because of the differences in both the test method and the definition of fracture toughness. Consider, for example, the 111 K test results. In the present investigation, fracture toughness was determined for crack initiation conditions. For the base metal, specimen failure occurred prior to pop-in, and the measured toughness is clearly indicative of the fracture resistance of the material under load-controlled conditions. However, in the HAZ tests, pop-in generally occurred, and the load and displacement at pop-in were used to determine the fracture toughness. In contrast, Sarno et al. measured fracture toughness under displacement-controlled conditions in accordance with the ASTM proposed R-curve procedure.<sup>17</sup>

Using these procedures, stable crack extension readily occurs prior to fracture, and toughness is measured after considerable crack extension has occurred. Since toughness increases following the initial increments of crack extension, the fracture toughness values determined by this method are higher.

In the HAZ tests on 38 mm (1½ in.) plate, Sarno<sup>18</sup> observed pop-in at approximately 110 MPa √m (100 ksi √in.) which is essentially the same as the value reported herein. However,

the test was continued until the full fracture resistance curve was developed, and a higher value of fracture toughness ( $217 \text{ MPa} \sqrt{\text{m}}$ ) was reported. Thus, the differences in fracture toughness results are attributable primarily to test method and not to material variability. Comments follow below on the significance of these differences from a design standpoint.

### Test Result Implications

The test data generated in this program indicate that for the conditions evaluated the fracture resistance of 5% Ni steel weldments may be significantly lower than expected on the basis of previous investigations.<sup>3,4</sup> In this section, the significance of the present results relative to LNG applications is assessed.

The fatigue crack growth rates in the HAZ for cracks growing through the thickness are 3 to 10 times faster than the rates reported by Sarno *et al*<sup>3</sup> for through-thickness cracks growing in the rolling direction. Consideration is given here to how these results influence life assessments based on fracture mechanics analysis. McCabe, Sarno and Feddersen<sup>19</sup> computed the number of fatigue cycles required to propagate an initial surface crack (semi-elliptical shape, 4 mm deep and 16 mm long, i.e.,  $5/32 \times 5/8$  in.) through the thickness of a 16 mm ( $5/8$  in.) thick plate of 5% Ni steel at 103 K.

The fatigue cycling conditions and the stress levels were appropriate for a semi-membrane tank in an LNG ship. Their analysis used the best-fit data of Sarno *et al*<sup>3</sup> for the base metal at 103 K ( $-274 \text{ F}$ ) as shown in Fig. 10. The results indicated that, assuming no crack growth retardation, the fatigue life of the initial flaw prior to leakage was approximately 192 years.

In this analysis, it was appropriate to use base metal data, because the crack growth rates were lower in the HAZ. The present results indicate that the growth rates are greater in the HAZ than in the base metal; however, the average rates in the HAZ still fall within the scatterband for the base metal defined by Sarno *et al*<sup>3</sup> and within the variability normally found in fatigue crack growth testing.<sup>20</sup> The upper bound line of Sarno *et al*<sup>3</sup> is a factor of 2.5 greater than the best-fit line used in the analysis,<sup>19</sup> i.e., the slope  $n$  of equation (8) is the same, but the  $C$  value is 2.5 times greater.

Use of the upper bound cracks growth data would conservatively account for the increased growth rates observed in the HAZ in the present study. Since life scales linearly with  $C$ , a conservative estimate of life based on the analysis of McCabe *et al*<sup>19</sup> but

using the present HAZ crack growth rates would be 77 years. Clearly, this life is sufficient for safe operation of LNG ships for their intended period of use is less than 30 years.

At 111 K the fracture toughness of the HAZ in the present study averaged  $108 \text{ MPa} \sqrt{\text{m}}$  at pop-in. In contrast, the HAZ toughness reported by Sarno *et al*<sup>3</sup> under displacement-controlled conditions was  $217 \text{ MPa} \sqrt{\text{m}}$  ( $196 \text{ ksi} \sqrt{\text{in.}}$ ) for 38 mm thick plate. The displacement-controlled toughness should be appropriate for redundant structures, but not for single load path structures such as storage tanks and the spherical shipboard tanks of the Moss-Rosenberg<sup>21</sup> design. The displacement-controlled toughness is a factor of 2 greater than the load-controlled toughness.

Since critical crack size scales as the square of fracture toughness, a four-fold decrease in critical crack size occurs under load-controlled conditions. Thus, the critical crack size of 102 cm (40.2 in.) calculated by Sarno *et al*<sup>3</sup> for a stress of 163 MPa (23.7 ksi) would be reduced to 25 cm (9.8 in.) for the present results. Measurements by Tenge and Solli<sup>22</sup> indicate that leaks are detectable at crack lengths of 2 to 4 cm (0.08 to 0.16 in.) on the penetrating side. Thus, there appears to be a reasonable margin of safety on critical crack size for the load-control case.

The preceding discussion suggests that the failure resistance of 5% Ni steel weldments is satisfactory for LNG applications. This is true for the uniform stress conditions evaluated. Further analyses are required to demonstrate structural safety for cases of combined membrane plus bending stresses. For combined loading, stress levels as high as 378 MPa (55 ksi) are permitted by the U.S. Coast Guard.<sup>23</sup> The higher stresses will result in faster crack growth rates and shorter critical sizes. In addition, the bending component will cause cracks to grow preferentially along the high tension surface, resulting in cracks that are much longer at the time of initial leakage. Assuming leakage still occurs prior to fracture, there is less time available for detecting the leak and taking preventive action than there would be for shorter cracks.

The results of the present investigation are also useful in deciding whether or not to substitute 5% Ni steel for 9% Ni steel. Substitution appears to be satisfactory for LNG applications where the service temperature is approximately 111 K. However, in liquid nitrogen at 76 K, the 5% Ni steel weldments exhibit brittle behavior and should not be used in place of 9% Ni steel which retains a higher level of toughness.<sup>1,5,16</sup> Since the scope of the current study was limited to evalua-

tion of a single weldment of 32 mm plate, care should be taken in using these data to justify selection of 5% Ni steel.

### Conclusion

The fatigue crack growth behavior and the fracture toughness of 32 mm thick 5% Ni steel weldments have been determined at room temperature, 111 K and 76 K.

The fatigue crack growth rates were determined for cracks propagating through the thickness. In this orientation, the crack growth rates in the base metal are essentially the same as previously reported for through-thickness cracks growing in the rolling direction. However, in contrast to previous results, the crack growth rates are faster in the HAZ than in the base metal, particularly at the lower temperatures.

Fracture toughness tests were conducted under load-controlled conditions using test material from the same heat of 5% Ni steel previously evaluated using controlled-displacement test conditions. In this investigation, the fracture toughness of the base metal at 111 K in the TL orientation averaged  $159 \text{ MPa} \sqrt{\text{m}}$  ( $144 \text{ ksi} \sqrt{\text{in.}}$ ), compared to a value of  $226 \text{ MPa} \sqrt{\text{m}}$  ( $204 \text{ ksi} \sqrt{\text{in.}}$ ) measured at 103 K in the controlled-displacement tests.

The fracture toughness of the HAZ ranged from 103 to 145 MPa  $\sqrt{\text{m}}$  (93 to 131 ksi  $\sqrt{\text{in.}}$ ) at 111 K, as compared to a value of 216 MPa  $\sqrt{\text{m}}$  (195 ksi  $\sqrt{\text{in.}}$ ) in the controlled displacement test. The differences in toughness were attributed to differences in the test methods employed and not to material variability.

The fatigue and fracture results reported herein suggest that 5% Ni steel is suitable for LNG applications, but more conservative estimates of life and critical crack size are in order. For the case of a semi-membrane tank subject to uniform membrane stresses, the estimated life prior to leakage and critical crack size are reduced by factors of 2.5 and 4, respectively, from values previously reported.

### Acknowledgments

This work was sponsored by the U.S. Maritime Administration; Mr. J. H. Seelinger was the project monitor.

The authors wish to thank D. A. Sarno and J. P. Bruner of the Armco Steel Company for providing the test weldment and the base metal characterization data. Appreciation is also expressed for R. L. Durholz of NBS who designed and fabricated the test dewar and R. L. Tobler, NBS, for critical review of this manuscript.



## References

1. Properties of Materials for Liquefied Natural Gas Tankage, ASTM STP 579, American Society for Testing and Materials 1975.
2. Pense, A. W., and Stout, R. D., "Fracture Toughness and Related Characteristics of the Cryogenic Nickel Steels," WRC Bulletin No. 205, Welding Research Council, May 1975.
3. Sarno, D. A., Bruner, J. P., and Kampschaefer, G. E., "Fracture Toughness of 5% Nickel Steel Weldments," *Welding Journal*, 53 (11), Nov. 1974, Res. Suppl., pp. 486-s to 494-s.
4. Bucci, R. J., Greene, B. N., and Paris, P. C., "Fatigue Crack Propagation and Fracture Toughness of 5 Nickel and 9 Nickel Steels at Cryogenic Temperatures," *Progress in Flaw-Growth and Fracture Toughness Testing*, ASTM STP 536, 1973, pp. 202-228.
5. Murayama, N., Pense, A. W., and Stout, R. D., "The Fracture Toughness of Cryogenic Steels," *Advances in Cryogenic Engineering*, Vol. 22, 1976.
6. Sarno, D. A., Chemical, Mechanical Property and Weldability Data of Armco CRYONIC 5 Steel, Armco Steel Company, June 1973.
7. Anon., U.S. Coast Guard Marine Engineering Regulations, Subchapter F, CG-115, July 1970.
8. Srawley, J. E., and Gross, B., "Stress Intensity Factors for Bend and Compact Specimens," *Engineering Fracture Mechanics*, Vol. 4, 1972, pp. 587-589.
9. McHenry, H. I., "A Compliance Method for Fatigue Crack Growth Studies at Elevated Temperatures," *Journal of Materials*, Vol. 6 (4), 1971, pp. 862-873.
10. Gross, B., Srawley, J. E., and Brown, W. F., Jr., "Stress Intensity Factors for a Single-Edge-Notch Tension Specimen by Boundary Collocation of a Stress Function," Technical Note D-2395, NASA, August 1964.
11. Landes, J. D., and Begley, J. A., "Test Results from J-Integral Studies—An Attempt to Establish a  $J_{IC}$  Testing Procedure," *Fracture Analysis*, ASTM STP 560, 1975, pp. 170-186.
12. Rice, J. R., Paris, P. C., and Merkle, J. G., "Some Further Results of J-Integral Analysis and Estimates," *Progress in Flaw-Growth and Fracture Toughness Testing*, ASTM STP 536, 1973, pp. 231-245.
13. Begley, J. A., and Landes, J. D., "The J-Integral as a Fracture Criterion," *Fracture Toughness*, ASTM STP 514, 1972, pp. 1-20.
14. Fowlkes, C. W., and Tobler, R. L., "Fracture Testing and Results for a Ti-6Al-4V Alloy at Liquid Helium Temperature," *Engineering Fracture Mechanics*, in press.
15. Paris, P. C., "The Fracture Mechanics Approach to Fatigue," *Proceedings, Tenth Sagamore Army Materials Research Conference*, Syracuse University Press, Syracuse, NY, 1964, pp. 107-127.
16. Tobler, R. L., Mikesell, R. P., Durholz, R. L., and Reed, R. P., "Low Temperature Fracture Behavior of Iron-Nickel Alloy Steels," Ref. 1, pp. 261-287.
17. Anon., Proposed Recommended Practice for R-Curve Determination, 1974 Annual Book of ASTM Standards, American Society for Testing and Materials, Philadelphia, PA, 1974.
18. Sarno, D. A., Armco Steel Corporation, Middletown, OH, private communication, 1976.
19. McCabe, D. E., Sarno, D. A., and Feddersen, C. E., "Fatigue Crack Growth Rate Studies of Partial Thickness Cracks in ASTM Method A645-74 5 Percent Nickel Steel," Ref. 1, pp. 238-260.
20. Clark, W. G., Jr., and Hudak, S. J., Jr., "Variability in Fatigue Crack Growth Rate Testing," Scientific Paper 74-1E7-MSLRA-P2, Westinghouse Research Laboratories, Pittsburgh, PA, September 18, 1974.
21. Howard, J. L., "LNG Marine Carrier Construction," *Marine Technology*, Vol. 9 (3), 1972, pp. 281-291.
22. Tenge, P., and Solli, O., "Fracture Mechanics in the Design of Large Spherical Tanks for Ship Transport of LNG," *Norwegian Maritime Research*, Vol. 1 (2), 1973, pp. 1-18.
23. Henn, A. E., and Dickey, T. R., "New Regulations for Liquefied Gas Carriers," paper presented at GASTECH 75, Paris, 1975.
24. Weston, W. F., Naimon, E. R., and Ledbetter, H. M., "Low Temperature Elastic Properties of Aluminum 5083-0 and Four Ferritic Nickel Steels," Ref. 1, pp. 397-420.

## WRC Bulletin 215 May 1976

### I "Development of Design Rules For Dished Pressure Vessel Heads"

by E. P. Esztergar

The present study is the continuation of an extensive investigation aimed at the development of rational design rules for formed pressure vessel heads. This problem was one of the first research projects the Design Division of PVRC selected for study and by maintaining its interest stimulated an increasing amount of work on the diverse behavior of seemingly similar head shapes. In the course of this work, not only new analysis techniques were developed but also a number of new failure modes unique to these deceptively simple looking geometrical shapes were uncovered.

### II "The Effect of Geometrical Variations on the Limit Pressures For 2:1 Ellipsoidal Head Vessels Under Internal Pressure"

by J. C. Gerdeen

This theoretical study has been conducted for the Subcommittee on Shells of the PVRC Design Division of the Welding Research Council. The impetus for this general study grew out of another specific study of the analysis of limit pressures of actual formed heads. Since it was found that actual formed heads are not uniform in thickness and that the thickness variations do affect the limit pressure, the thickness variation was studied in detail using a computer analysis that included bending theory.

Publication of these papers was sponsored by the Pressure Vessel Research Committee of the Welding Research Council.

The price of WRC Bulletin 215 is \$8.00 per copy. Orders should be sent with payment to the Welding Research Council, United Engineering Center, 345 East 47th Street, New York, N.Y. 10017.